RSC Advances

ROYAL SOCIETY OF CHEMISTRY

www.rsc.org/advances

Cite this: DOI: 10.1039/c0xx00000x

www.rsc.org/xxxxxx

ARTICLE TYPE

Novel supramolecular assemblies of repulsive DNA-anionic porphyrin complexes based on covalently modified multi-walled carbon nanotubes and cyclodextrins

Jingheng Ning,[a,c] Yufang Wang,[b] Qi Wu,[a] Xuefeng Zhang,[c] Xianfu Lin*[a] and Hongbin Zhao*[b]

Received 3rd December 2014, Accepted Xth XXXXXXXXX 2015
DOI: 10.1039/b000000x

We have prepared the water-soluble anionic 5-(p-aminophenyl)-10,15,20-tri(p-sulfonatophenyl)porphyrin (ATSPP) for constructing novel supramolecular assemblies of DNA-anionic porphyrin complexes. ATSPP was covalently linked to multi-walled carbon nanotubes (MWCNTs) to give a suspension of a conjugate (ATSPP-MWCNTs) that was stable for >2 weeks. On addition of cyclodextrins (CDs), the corresponding complex (ATSPP-MWCNTs-CDs) was further formed. Absorption and fluorescence spectra displayed that 1:1 inclusion complexes were formed with either α-CD or β-CD, but that virtually no interaction occurred with γ-CD. A comparative study on the interaction of DNA with ATSPP-MWCNTs and the ATSPP-MWCNTs-CDs complexes was carried out by fluorescent spectroscopy, resonance light-scattering, and transmission electron microscopy. Results showed that negatively-charged ATSPP-MWCNTs can interact with the negatively charged DNA, indicating that covalently modified CNTs contribute to the counterintuitive binding of anionic porphyrins with DNA. This can be possibly attributed to π-stacking interactions between sidewalls of CNTs and bases in DNA. Secondly, ATSPP-MWCNTs-CDs complexes interact better with DNA than the ATSPP-MWCNTs, indicating that CDs can promote the binding of DNA to anionic porphyrins covalently modified MWCNTs. This is probably due to the fact that the amphiphilic CDs can greatly improve the solubility and dispersity of ATSPP-MWCNTs by their effective inclusion complexation with ATSPP. The successful construction of the supramolecular assemblies ATSPP-MWCNTs-CDs-DNA provides a new approach to binding anionic porphyrins to negatively charged DNA.

Introduction

Interactions of porphyrins with DNA have been widely reported and porphyrin-DNA complexes have been applied in various biological and medical fields, such as DNA detection and recognition,[1] and tumor therapy.[2] Schlepping with negative charges and grooves on its main chain, DNA preferentially interacts with substrates bearing positive charges or highly π-conjugated groups through electrostatic attractions or π-stacking interactions.[3] Owing to the structural motifs such as positive-charged peripheral groups and macrocyclic aromatic core, the representative of cationic porphyrins, meso-tetra(N-methylpyridinium-4-yl)porphyrin (TMpyP) and its derivatives, have been verified to exhibit good affinity with DNA.[1-7] In contrast, anionic porphyrins are generally believed not apt to "naturally bind" DNA due to the inherent electrostatic repulsions caused by negative charges,[8] and researches in this field are scarce. Nevertheless, interactions of anionic porphyrins and DNA still attract much attention, basing on the following points. Firstly, anionic porphyrins have the same macrocylic aromatic core (porphine ring) as that of cationic ones, and the π-π interactions which are similar to those between cationic porphyrins and DNA may also occur between anionic ones and DNA. These π-π interactions may offer possibility to bind anionic porphyrins with DNA successfully, because they can be strengthened to overcome the electrostatic repulsions. On the other hand, anionic porphyrins have negative-charged groups (e.g., nido-carboranyl, SO_3^- or COO^-)[9-11] that are quite different from those of cationic ones, and so may show different properties and behaviors when interacting with DNA, which will give an opportunity to develop novel porphyrin-DNA complexes for interesting and promising applications.

In recent years, researchers have been focused on developing easy and effective methods for achieving counterintuitive but doable interactions between anionic porphyrins and DNA. Purrello reported that DNA could interact well with anionic nido-carboranyl porphyrins, attributed to both the porphyrin inner core protonation to reduce electrostatic repulsions and a non-covalent interaction caused by chirality match between them.[12] Besides, protonated reagent like spermine was used as a positive-charged mediator to remarkably shield electrostatic repulsions between sulfonated nickel(II) porphyrin and Z-DNA, forming a stable anionic porphyrin-Z-DNA complex that could be applied for spectroscopical discrimination of Z-DNA.[13, 14] It is necessary to

point out that there was another synergetic interaction contributing to the stability of that complex, which was the axial coordination between nitrogen N7 of guanine in Z-DNA and central metal nickel (II) in the middle of porphine ring. Thus, as demonstrated by these findings, reducing inherent electrostatic repulsions along with increasing non-electrostatic interactions should be considered as a feasible strategy to facilitate anionic porphyrin interactions with DNA.

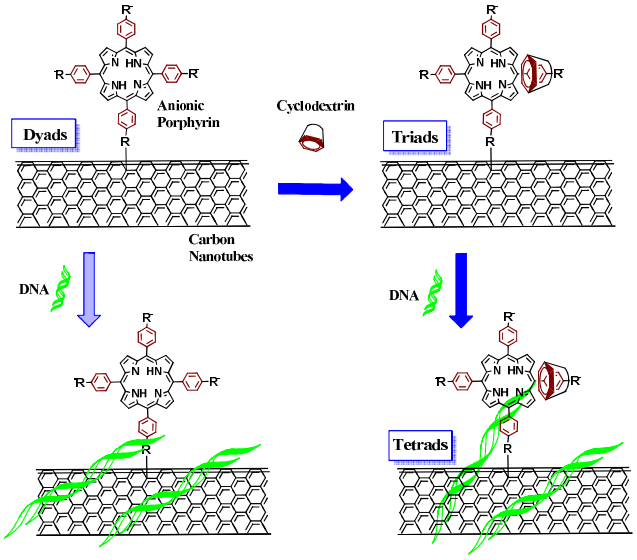

Scheme 1. The strategy for constructing novel DNA-anionic porphyrin supramolecular assemblies by the "fixation" of CNTs and the "inclusion" of CDs.

It is well known that carbon nanotubes (CNTs) can bind to DNA through π-stacking interactions,[15] and can be modified by porphyrins to improve dispersity for applications.[16-18] Thus, by connecting CNTs to anionic porphyrins, the former will endow the latter with a very large π-conjugated structure, which probably enable the originally repelled latter to interact counterintuitively but well with DNA for a great increase of π-π interactions. On the other hand, with a special amphiphilic structure, cyclodextrins (CDs) can mediate DNA interactions with organic functional molecules *via* supramolecular inclusion complexation,[19] and may include peripheral substituents at the porphyrin ring inside their hydrophobic cavities.[20-23] Thus, through the introduction of CDs, the CNTs modified with anionic porphyrins will probably interact with DNA better for a possible decrease of electrostatic repulsions, attributed to the fact that CDs can include phenyl rings of porphyrin into their hydrophobic cavities to keep sulfonato groups away from DNA and so reduce electrostatic repulsions between them. Therefore, in the present study, we could follow a strategy by selecting CNTs and CDs as two fascinating candidates helpful to form stable DNA-anionic porphyrin complexes. The main route could be described as follows (**Scheme 1**): from the initial anionic porphyrin to anionic porphyrin-CNTs dyads, and then to anionic porphrin-CNTs-CDs triads, and finally transformed into the targeted anionic porphyrin-CNTs-CDs-DNA tetrads that have not yet been reported to the best of our knowledge. This strategy would have high feasibilities since it was based on our previous work in the field of porphyrin interactions with CNTs[16, 17] or CDs.[20, 21] Moreover, the tetrad "anionic porphyrin-CNTs-CDs-DNA" would combine the outstanding merits of the "two fascinating candidates", such as (i) non-toxicity, (ii) good biocompatibility, (iii) unusual capability to penetrate cell membranes to serve as gene delivery systems (CNTs),[24] (iv) extraordinary amphiphilicity to improve solubility of "guest molecules" and overcome their aggregation in solution (CDs).[25] Therefore, the current work will surely enrich the research on porphyrin-DNA complexes and may lay novel foundations for promising biological or medical applications.

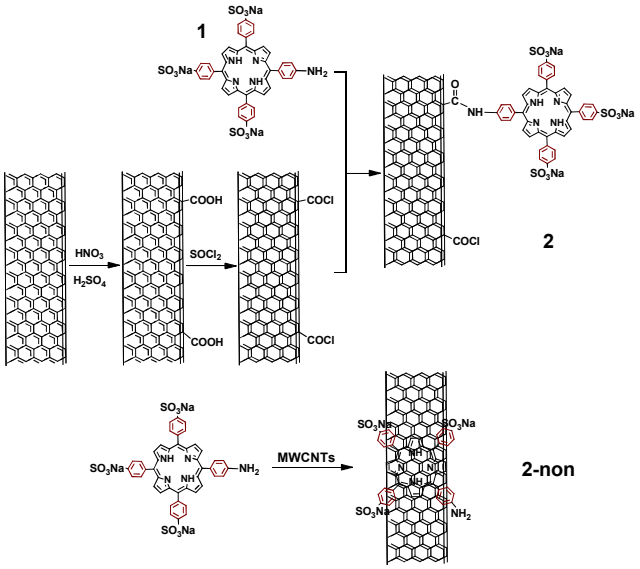

Scheme 2. Synthesis of ATSPP-MWCNTs **2** and ATSPP-π-π-MWCNTs **2-non**

Experimental

Reagents and apparatus

MWCNTs were purchased from Shenzhen Bill Technology Development Ltd. (Shenzhen, China) and used without further purification. α-CD and γ-CD were purchased from Shanghai Sangon Biotech Co., Ltd. (Shanghai, China), and β-CD was purchased from Shanghai Chemical Reagent Factory (Shanghai, China). Calf thymus DNA (*ct*-DNA) was purchased from Livzon Pharmaceutical Group Inc (Zhuhai, China). A buffer solution (pH 7.04) of Na_2HPO_4–KH_2PO_4 was freshly prepared. N,N-dimethyl formamide (DMF) was freshly distilled from anhydrous calcium sulfate. All chemicals were of analytical grade and water was double distilled.

^{1}H NMR spectrum was recorded in a DMSO-d_6 solution at 25 □ on a Varian Mercury Plus 400 (Varian, USA). FT-IR spectrum was obtained with a BRUKER TENSOR 27 instrument (Bruker Optics, Germany), and the sample was prepared with use of KBr of spectroscopic grade. The absorption spectra were measured on a La 25 UV/vis spectrometer (PerkinElmer, USA), while the fluorescence and RLS spectra were measured on a Ls-55 fluorescence spectrometer (PerkinElmer, USA), and all the experiments were carried out in the aqueous solution. Thermogravimetric analyses (TGA) were conducted on a TG-60

instrument (Shimadzu, Japan), under a flowing air at a scanning rate of 20 °C/min from room temperature to 800 °C. The TEM images were obtained with a JEM-3100 transmission electron microscope (JEOL, Japan).

Preparation of 2

Porphyrin **1** was prepared according to the literature.[26] Then ATSPP-MWCNTs **2**, a complex of porphyrin covalently modified multi-walled carbon nanotubes, was synthesized by a procedure described in **Scheme 2**. MWCNTs were purified and oxidized with a mixture of concentrated sulfuric and nitric acid (3:1, 98% and 70%, respectively) at 80 °C under sonication for 8 h. The resulted MWCNT-COOH (20 mg) was refluxed in 20 mL of thionyl chloride at 70 °C for 72 h. After removing the excess thionyl chloride under vacuum, the residue was re-dispensed in 10 mL of DMF, then 20 mg of **1** was added, and the resulted mixture was stirred at 100 °C for 72 h under Argon atmosphere. After the reaction finished, DMF was removed and 20 mL of water was added. Then, through filtration, the sediment was washed with 60 mL of water to remove the unreacted porphyrin. The crude product was purified by centrifugation, and dried at 40 °C for 10 h under vacuum. Finally, the desired black solid of **2** was obtained. ATSPP-π-π-MWCNTs **2-non**, the complex of porphyrin non-covalently modified multi-walled carbon nanotubes, was obtained also as a black solid according to the procedure similar to the above, by using pristine MWCNTs without any treatment, at the room temperature and without Argon protection (**Scheme 2**).

Interaction investigations

To investigate the inclusion interaction of **2** with CDs, 1.0 mL of the stock solution (9.0×10^{-2} g L^{-1}) of **2** was transferred into a 10-mL volumetric flask, and then the CDs solution (1.5×10^{-2} mol L^{-1}) was added with the volume ranging from 0 μL to 80 μL. The mixed solution was diluted to final volume with double distilled water, and the pH was fixed at 7.04 with a 0.2 mol L^{-1} phosphate buffer solution. After being shaken thoroughly, it was determined in 10 min at 25±1 °C.

To investigate the interaction of **2** with DNA and the influence of CDs during this process, at first, 1.0 mL of the stock solution (9.0×10^{-2} g L^{-1}) of **2** was transferred into a 10-mL volumetric flask in the absence or presence of 80 μL of CDs solution (1.5×10^{-2} mol L^{-1}). Then, an appropriate amount of 2.0×10^{-3} mol L^{-1} *ct*-DNA solution was added with the volume ranging from 0 μL to 72 μL. The mixed solution was diluted to final volume with double distilled water, and the pH was fixed at 7.04 with a 0.2 mol L^{-1} phosphate buffer solution. After being shaken thoroughly, it was determined in 10 min at 25±1 °C.

Results and Discussion

Characterization of 1, 2 and 2-non

The structure of ATSPP **1** was confirmed by ^{1}H NMR (**Figure S1, Electronic Supplementary Information, ESI**). Both ATSPP-MWCNTs **2** and ATSPP-π-π-MWCNTs **2-non** were soluble in H_2O, DMF and ethanol, and the formed black solution of **2** or **2-non** could keep stable for more than two weeks or about six days, respectively, which was favourable for the following reactions and characterizations. These results indicated the solubility or dispersity of MWCNTs can be improved by either covalent or non-covalent modification with water-soluble ATSPP; however, the covalent way might be preferable since **2** was found to exhibit better dispersity and stability than **2-non**. In the FT-IR spectrum of **2**, the characteristic absorptions at 1642 and 1050 cm^{-1} could be assigned to the stretching vibration of the amide C=O bond and its C-N bond, respectively (**Figure S2, ESI**). It indicated that **1** was successfully covalently attached to the surface of the MWCNTs with an amide bond by the method shown in **Scheme 2**. In the spectrum of **2-non**, the small shoulder peak on the left side of 1642 cm^{-1} (another characteristic absorption for the C=O bond) could not be observed (**Figure S2, ESI**), which indicated that there wasn't a carbonyl group in **2-non** and **1** was absorbed onto MWCNTs surface in a non-covalent way (π-π interaction) as shown in **Scheme 2**.

In the UV-vis spectra, the absorption of **2** in H_2O showed a Soret band at 423 nm (for **2-non**, 415 nm) and a broad signal monotonical decrease in the range of 300-800 nm, corresponding separately to the attached porphyrin and the multi-walled carbon nanotubes (**Figure 1a**). Compared to the absorption spectrum of **1** (the Soret band: 412 nm), the spectrum of **2** showed a red-shift of the Soret band as big as 11 nm (for **2-non**, as small as 3 nm), without seeing the Q-bands due to the overwhelmingly broad absorption of MWCNTs. The phenomenon observed here gave strong support for the covalent attachment of porphyrins to MWCNTs in Complex **2** and the non-covalent absorption of porphyrins on MWCNTs in Complex **2-non**, since non-covalently attached porphyrins on CNTs could not cause a large shift of the Soret band, as previously reported.[27] In the fluorescence spectra, upon the excitation of the porphyrin moiety at the Soret band (423 nm), the solution of **2** exhibited about 80-90% quenching of emission bands at 654 and 716 nm, as compared to that of **1** at a matching absorption (**Figure 1b**). The fluorescence spectrum of **2-non** was similar to that of **2**, but with a slightly stronger quenching. This might be explained by the different distance from porphyrin to CNTs in the different complexes.[17] In **2-non**, the porphyrin molecule could be kept very close to the CNTs surface by π-π stacking like "face-to-face", which was favourable for the electron transferring process and so caused a stronger fluorescence quenching; in **2**, the amide bond meant a relatively longer distance from porphyrin to CNTs, which led to a more difficult electron-transfer process and finally a relatively smaller quenching degree. Nevertheless, all of these results support the presence of an electron-transfer process from

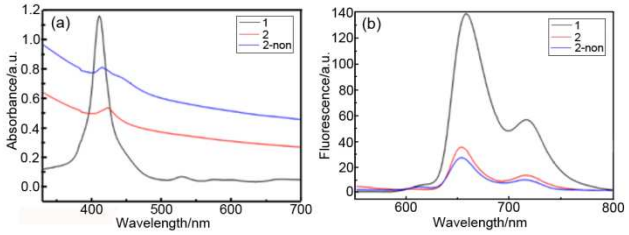

Figure 1. (a) The absorption spectra of ATSPP **1**, ATSPP-MWCNTs **2** and ATSPP-π-π-MWCNTs **2-non** (C_{ATSPP}, 1.0×10^{-6} mol L^{-1}; $C_{ATSPP\text{-}MWCNTs}$, 5.0×10^{-2} g L^{-1}; $C_{ATSPP\text{-}\pi\text{-}\pi\text{-}MWCNTs}$, 5.0×10^{-2} g L^{-1}). (b) The fluorescence spectra of ATSPP **1**, ATSPP-MWCNTs **2** and ATSPP-π-π-MWCNTs **2-non** (C_{ATSPP}, 1.0×10^{-7} mol L^{-1}; $C_{ATSPP\text{-}MWCNTs}$, 3.0×10^{-3} g L^{-1}; $C_{ATSPP\text{-}\pi\text{-}\pi\text{-}MWCNTs}$, 3.0×10^{-3} g L^{-1}).

ATSPP to MWCNTs, which proved MWCNTs could be modified by ASTPP successfully in either a covalent or a non-covalent way. Besides, the TGA curve of **2** showed no clear "major" weight loss but only a "gradual" one over the temperature range corresponding to the porphyrin (**Figure S3, ESI**), reflecting the absence of free porphyrins (herein, **1**) in the sample (herein, **2**), and in turn, providing an evidence for the covalent linkage of **1** with MWCNTs.

Construction and confirmation of the inclusion complexes 3

In order to investigate the influence of CDs on the interaction between DNA and **2**, two kinds of **3** (ATSPP-MWCNTs-α-CD **3a** and ATSPP-MWCNTs-β-CD **3b**) were constructed. Inclusion abilities of different CDs with **2** and their inclusion constants were further determined by fluorescence spectrometry. **Figure 2** showed changes in the fluorescence characteristics of **2** in the KH_2PO_4–K_2HPO_4 buffer solution (pH 7.04) at various concentrations of α-CD and β-CD. The fluorescence excitation bands were fixed at 423 nm. Along with the increasing concentration of α-CD or β-CD, the fluorescence intensity of the emission bands at 654 nm decreased gradually, which illustrated the formation of the inclusion complexes **3**.

The inclusion constant (K) is an important parameter, which represents the inclusion capacity. K can be obtained from fluorescence data by the modified Benesi-Hildebrand equation.[28]

$$\frac{1}{F - F_0} = \frac{1}{K k Q [P]_0} \times \left(\frac{1}{[CD]_0^n} + \frac{1}{kQ[P]_0}\right)$$

Herein, F and F_0 represented the fluorescence intensities of **2** in the presence and absence of CDs, respectively. $[P]_0$ denoted the initial concentration of **2** and $[CD]_0$ denoted that of CDs. k was the instrument constant, and Q was the fluorescence quantum yield of the inclusion complex. K, the inclusion constant of **3**, was determined by doubled reciprocal method. $1/(F-F_0)$ versus 1/[CD] was plotted and K was obtained from the ratio of the intercept to the slope. According to this formula, the K values for the inclusion complexes of α-CD and β-CD with **2** were calculated as 5.3×10^3 M^{-1} and 3.1×10^3 M^{-1}, respectively, with the same stoichiometry of 1:1. However, when similar experiments were performed under the same conditions by using γ-CD, few changes of fluorescence spectra could be observed, indicating there was no interaction between γ-CD and **2**. These results showed that α-CD and β-CD could include ATSPP-MWCNTs **2** while γ-CD could not, and the inclusion ability of α-CD was stronger than that of β-CD. As is well known, these three kinds of CDs have no difference in the molecular structure except for the number of glucose units, resulting in different molecular dimensions. Among them, α-CD has a hydrophobic cavity of the smallest size (α-CD: 13.7/5.7 Å; β-CD: 15.3/7.8 Å; γ-CD: 16.9/9.5 Å), which is closest to that of the phenyl group (about 5.8 Å). Meanwhile, "size matching" is known to be the first important factor for determining the stability of CDs inclusion complexes.[22] Since the peripheral substituent of **2** (sulphonatophenyl) was small for the cavity of γ-CD, it would easily pass in and out the cavity with little bonding. Thus, in the present work, α-CD was found to be able to best include **2** and form the most stable complex ATSPP-MWCNTs-α-CD **3a**.

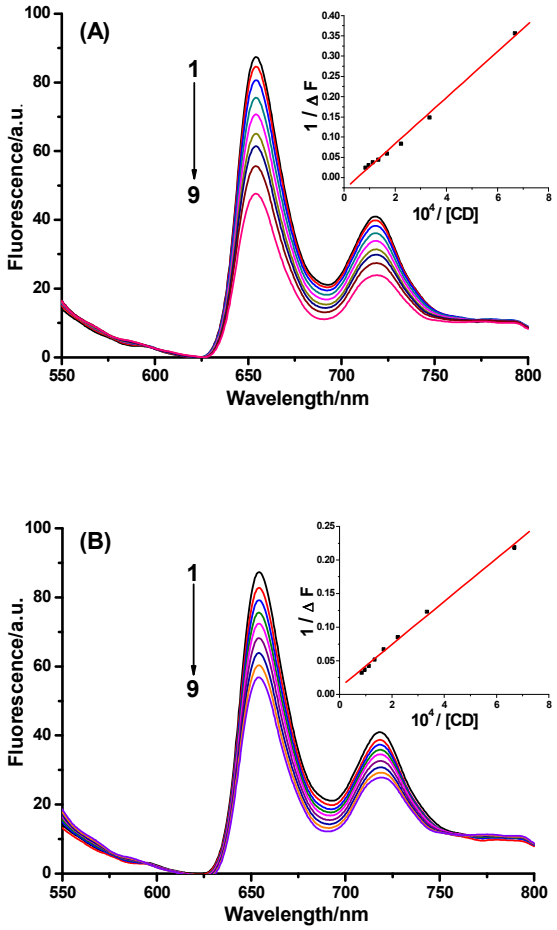

Figure 2. The fluoresence spectra of **2** (9×10^{-3} g L^{-1}) in the pH 7.04 phosphate buffer solution containing various concentration of (A) α-CD (B) β-CD at 25 °C (excitation wavelength 423 nm). The concentration of CD is: (1) 0 M; (2) 1.5×10^{-5} M; (3) 3.0×10^{-5} M; (4) 4.5×10^{-5} M; (5) 6.0×10^{-5} M; (6) 7.5×10^{-5} M; (7) 9.0×10^{-5} M; (8) 1.05×10^{-4} M; (9) 1.2×10^{-4} M. Inset: the linear plot of $1/(F-F_0)$ versus 1/[CD].

By contrast, two kinds of inclusion complexes **3-non** (ATSPP-π-π-MWCNTs-α-CD **3a-non** and ATSPP-π-π-MWCNTs-β-CD **3b-non**) together with two kinds of inclusion complexes **3-por** (ATSPP-α-CD **3a-por** and ATSPP-β-CD **3b-por**) were constructed in the same way as above-mentioned. The changes in the fluorescence characteristics of **2-non** or ATSPP in the KH_2PO_4–K_2HPO_4 buffer solution (pH 7.04) at various concentrations of α-CD and β-CD were shown in **Figure S4 (ESI)** or **Figure S5 (ESI)**, respectively. And similarly, no change could be observed when using γ-CD. The K values for the inclusion complexes **3a-non**, **3b-non**, **3a-por** and **3b-por** were calculated as 1.4×10^3 M^{-1}, 8.9×10^2 M^{-1}, 7.2×10^3 M^{-1} and 6.4×10^3 M^{-1}, respectively, with the same stoichiometry of 1:1. Compared to the interaction between CDs and **2**, there were a lot of similarities in the interaction between CDs and **2-non** or the free porphyrin ATSPP, such as: (i) the changes of the fluorescence intensity

shown in **Figure S4 (ESI)** or **Figure S5 (ESI)** decreased gradually in the same way as shown in **Figure 2**, and the emission bands were also peaked at 654 nm; (ii) **2-non** or ATSPP could be included by α-CD and β-CD, but not by γ-CD; (iii) α-CD could include **2-non** or ATSPP better than β-CD, and all of their stoichiometries were the same 1:1. Besides, the value of their inclusion constants K changed regularly with the included (guest) compounds accordingly: $K_{3a\text{-}por} > K_{3a} > K_{3a\text{-}non}$; $K_{3b\text{-}por} > K_{3b} > K_{3b\text{-}non}$. Obviously, as a guest compound for CDs, the free porphyrin ATSPP could be the best one, the covalent complex (ATSPP-MWCNTs) was the second, while the non-covalent complex (ATSPP-π-π-MWCNTs) was the worst. The reason might be as follows: (i) once the water-soluble ATSPP was complexed with the insoluble MWCNTs, the originally good compatibility between the free porphyrin and CDs would decrease significantly, and meanwhile between them, a steric hindrance caused by the bulky MWCNTs would arise immediately. So the free porphyrin ATSPP could interact better with CDs than ATSPP-MWCNTs or ATSPP-π-π-MWCNTs; (ii) in the non-covalent complex the porphyrin molecule could be kept very close to the CNTs surface, while in the covalent complex there might be a relatively longer distance between ATSPP and MWCNTs due to the amide bond, so the steric hindrance between ATSPP-π-π-MWCNTs and CDs would be greater than that between ATSPP-MWCNTs and CDs. Moreover, ATSPP-π-π-MWCNTs showed poorer stability and dispersity than ATSPP-MWCNTs. Thus, the covalent complex ATSPP-MWCNTs could interact better with CDs than the non-covalent complex ATSPP-π-π-MWCNTs.

Construction of supramolecular assemblies based on 2 or 3

Based on the investigation of the interactions between **2** and CDs, comparative studies on DNA interactions with **2** and **3** were also carried out, respectively. To the best of our knowledge, no researches concerning DNA condensation with anionic porphyrin covalently modified CNTs have been reported. Thus, it is valuable to investigate whether DNA can interact with the complex **2**, in which the anionic porphyrin has been "fixed" onto the surface of the π-conjugated MWCNTs *via* a covalent bond. In current experiments, upon the addition of various concentration of DNA (0-72 μL) into the aqueous solution of **2**, the fluorescence spectrum of **2** exhibited about 25±0.26% (n=6) quenching of emission bands at 654 and 716 nm (**Figure 3A**), indicating that the interaction between DNA and **2** happened indeed. Additionally, contrasted experiments were performed by using ATSPP **1** or **2-non** and few changes of fluorescence spectra were observed, indicating there was no interaction between DNA and **1** (or **2-non**) (**Figure S4** or **Fugure S5**, **ESI**: dotted line 1 in the left inset). These results attested that CNTs could facilitate the binding of the negative-charged porphyrin with the negative-charged DNA, as expected, but only when they were "covalently" modified by anionic porphyrin. It was probably since (i) the anionic porphyrin in the complex **2** was "fixed" firmly on the surface of the carbon nanotubes *via* a stable covalent bond, resulting in less contact with DNA and so less repulsions, (ii) in the complex **2**, the CNTs bearing the anionic porphyrin could non-covalently interact with DNA owing to π-stacking interactions between the sidewalls of CNTs and the bases in DNA.[15] But in the complex **2-non**, CNTs had already non-covalently interacted with the anionic porphyrin by π-π stacking and some of their surfaces were "covered" with "free" anionic porphyrin molecules, so that they had less space for DNA and their "anionic-porphyrin-covered" surface would even show up great resistance against DNA due to the electrostatic repulsions. Herein, by covalently linking **1** with MWCNTs to form **2**, the inherent electrostatic repulsions between **1** and DNA might be reduced, and the π-stacking interactions existing between CNTs and DNA could cause the binding of **2** with DNA successfully.

Further experiments were performed to investigate the interaction between DNA and **3** as well as to study the influence of CDs in this process. **Figure 3B** and **3C** displayed the changes of fluorescence spectra when DNA solution (0-72 μL) was gradually added into the aqueous solution of **2** in the presence of α-CD and β-CD, respectively, under the same experimental conditions. In **Figure 3B** and **Figure 3C**, a gradual decrease of the fluorescence intensity of emission bands peaked at 654 nm could be observed, with a quenching about 74±0.32% of **3a** and 46±0.29% of **3b**, respectively. The difference was significant ($n=6$, $p \leq 0.05$, t test, two sides). It suggested that both **3a** and **3b** could interact with DNA to construct the corresponding supramolecular assemblies ATSPP-MWCNTs-α-CD-DNA **4a** and ATSPP-MWCNTs-β-CD-DNA **4b**. Thus, **3a** as well as **3b** exhibited a relatively stronger affinity for DNA than **2** (the fluorescence quenching is about 25%), indicating that these two kinds of CDs could promote the interaction between DNA and **2** as expected. At the same time, **3a** exhibited a greater degree of emission quenching than **3b**, implying its relatively stronger binding affinity for DNA in line with its stronger inclusion capability of **2**. However, when control experiments were performed under the same conditions to investigate the interaction between DNA and **3-non** or **3-por**, few changes of fluorescence spectra could be observed, indicating there was no interaction between DNA and **3-non** or **3-por** (including both **3a-por** and **3b-por**) (**Figure S4** or **Figure S5**, **ESI**: dotted line 8 and 9 in the left inset). The results indicated that CDs could promote the binding of DNA with ATSPP only when ATSPP was covalently modified onto the MWCNTs surface. Obviously, in the inclusion complex **3-por**, although CDs could include phenyl rings inside their hydrophobic cavities and might isolate sulfonato groups from DNA to reduce their repulsions to a certain extent, the electrostatic repulsions between DNA and **3-por** were still strong enough to prevent them from binding. But once the anionic porphyrin was "fixed" onto MWCNTs, as mentioned, based on a strong π-stacking interaction between CNTs and DNA, a stable supramolecular assembly including both anionic porphyrin and negative DNA would be successfully constructed; and in this case, amphiphilic CDs could effectively improve the solubility and dispersity of ATSPP-MWCNTs and the stability of ATSPP-MWCNTs-DNA and so promote the final formation of the complex ATSPP-MWCNTs-CDs-DNA.

Recently, resonance light-scattering (RLS) has been regarded as a useful tool for the investigation of supramolecular complexes.[30] The amount of scattered light is directly proportional to the volume of particles, and monomeric molecules or small oligomers do not show enhanced scattering.[31] Herein, RLS technology was used to detect the interaction between DNA and **3**. Prior to the addition of DNA,

the RLS of ATSPP-MWCNTs-α-CD **3a** was mono-exponential, and its special profile was determined (**Figure 4**, line 1, black). Upon the addition of different amounts of DNA (4-12 μL, 2×10^{-3} M), the RLS intensity changed from 450 to 990, implying the formation of the supramolecular assembly ATSPP-MWCNTs-α-CD-DNA **4a** (**Figure 4**, line 2-4).

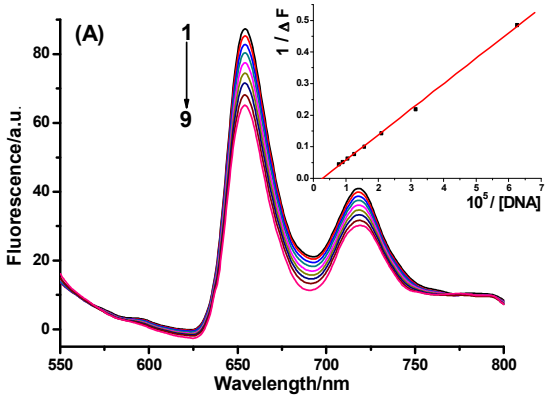

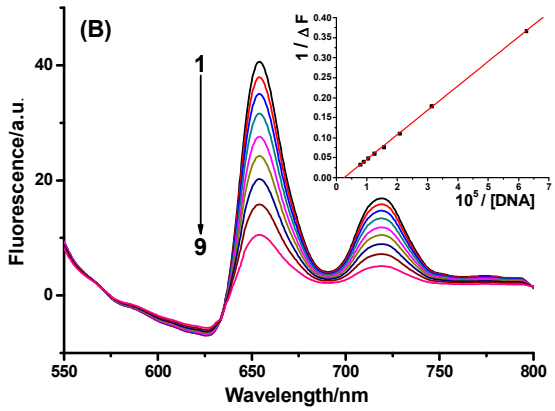

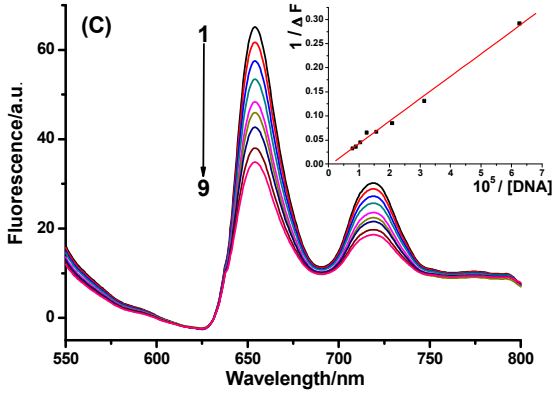

Figure 3. The fluoresence spectra of **2** (9×10^{-3} g L^{-1}) in the pH 7.04 phosphate buffer solution containing various concentration of DNA in the presence of (A) 0 μL CD (B) 80 μL α-CD (1.2×10^{-4} M) (C) 80 μL β-CD (1.2×10^{-4} M) at 25 ºC (excitation wavelength 423 nm). The concentration of DNA is: (1) 0 M; (2) 1.8×10^{-6} M; (3) 3.6×10^{-6} M; (4) 5.4×10^{-6} M; (5) 7.2×10^{-6} M; (6) 9.0×10^{-6} M; (7) 1.08×10^{-5} M; (8) 1.26×10^{-5} M; (9) 1.44×10^{-5} M. Inset: the linear plot of $1/(F-F_0)$ versus 1/[DNA].

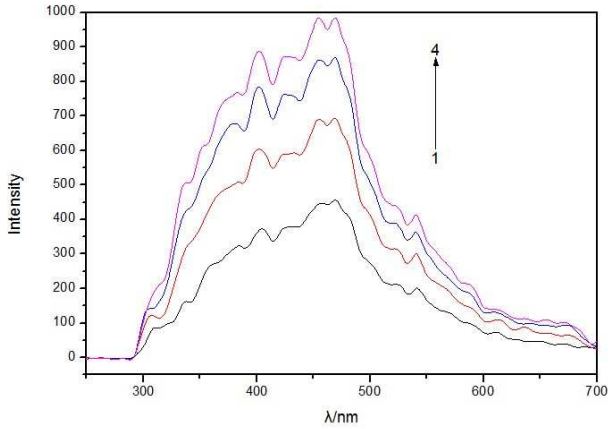

Figure 4. The RLS spectra of **3a** solution in (1) 0 μL (2) 4 μL (3) 8 μL (4) 12 μL of DNA (2×10^{-3} M).

The morphology of MWCNTs, **2**, **3a** and **4a** was observed by TEM, providing direct evidences for the whole formation process of **4a**. **Figure 5A** showed the unmodified MWCNTs, and we could see the MWCNTs wall was very smooth. In contrast, the surfaces of dyad **2** showed a thick coverage (about 2.7 nm) of porphyrin **1** on the sidewalls of MWCNTs, indicating that MWCNTs were modified by ATSPP (**Figure 5B**). A similar observation was found for **3a** in **Figure 5C**, and the thickness of the layer attached on the carbon nanotubes was about 3.4 nm. From **2** to **3a**, the thickness increase of the layer as shown in **Figure 5B** and **Figure 5C** was basically in conformity with the size of α-CD.[22] In **Figure 5D**, there were clearly a thicker layer (about 5 nm) attached on MWCNTs, which suggested the thick coverage of DNA onto the sidewalls of MWCNTs moiety of **3a**.

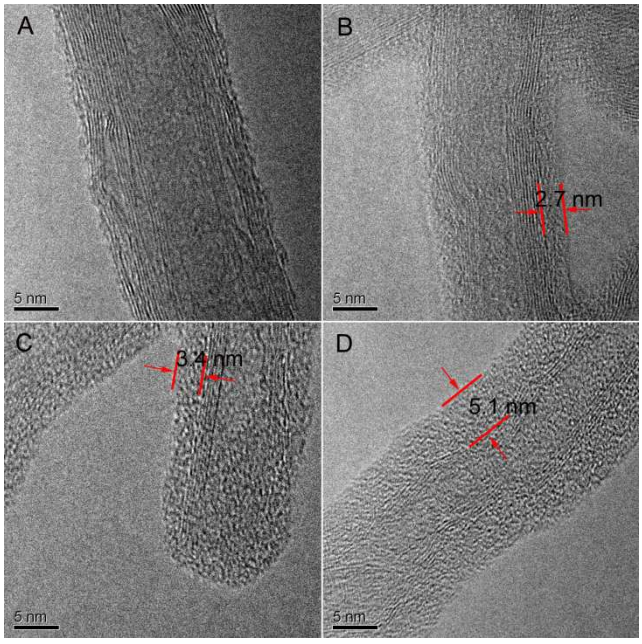

Figure 5. TEM photomicrographs of (A) MWCNTs **1**; (B) ATSPP-MWCNTs **2**; (C) ATSPP-MWCNTs-α-CD **3a**; and (D) ATSPP-MWCNTs -α-CD-DNA **4a**

Conclusions

In this paper, based on water-soluble anionic 5-(p-aminophenyl)-10,15,20-tri(p-sulphonatophenyl)-porphyrin (ATSPP) **1**, two nanocomposites, ATSPP-MWCNTs dyad **2** and ATSPP-MWCNTs-CDs triad **3** were prepared. Using these two nanocomposites to interact with DNA respectively, the corresponding supramolecular assemblies ATSPP-MWCNTs-DNA and the targeted ATSPP-MWCNTs-CDs-DNA tetrad **4** were successfully constructed, and the effects of CNTs or CDs on the binding of DNA with anionic porphyrins were studied in detail through UV/vis, fluorescence, RLS and TEM. By contrast, a series of complexes, ATSPP-π-π-MWCNTs **2-non**, ATSPP-π-π-MWCNTs-CDs **3-non** and ATSPP-CDs **3-por** were prepared, and control experiments were performed to investigate their interactions with DNA. Results showed that both CNTs and CDs are favourable for the construction of supralomolecular assemblies containing the negative-charged anionic porphyrin **1** and the negative-charged DNA. However, CNTs could facilitate the anionic porphyrin binding with DNA by increasing π-π interactions, only when they were covalently modified by anionic porphyrin; while CDs could only promote the interaction between DNA and ATSPP-MWCNTs, probably by greatly improving the solubility and dispersity of ATSPP-MWCNTs based on the effective inclusion complexation of CDs with ATSPP. Our present work developed a new route for the construction of anionic porphyrin-DNA complexes *via* supramolecular assembling, which was significant for the advancement of porphyrin-DNA chemistry and their promising applications in drugs and clinical therapies. Further studies on the interaction mechanisms between anionic porphyrins and repulsive DNA are in progress in our laboratory.

Acknowledgments

Authors gratefully acknowledge financial support from the National Natural Science Funds for Young Scholar of China (No.31301564), the Projects in the National Science & Technology Pillar Program during the Twelfth Five-Year Plan Period (No.2012BAD31B08), Hunan Provincial Natural Science Foundation (No.2015JJ2011) and Hunan Provincial Engineering Research Center for Food Processing of Aquatic Biotic Resources (No.2015GCZX004), Changsha University of Science & Technology, PR China.

Author Address

*[a]*Department of Chemistry, Zhejiang University, Hangzhou, Zhejiang 310027, P. R. China. Fax: + 86 571 87952618; Tel: + 86 571 87951588; E-mail: llc123@zju.edu.cn*

[b]College of Chemistry and Environmental Engineering, Dongguan University of Technology, Dongguan, Guangdong 523808, P. R. China. Fax: + 86 731 85040753; Tel: + 86 135 74806898; E-mail: zhaohbhanlf@163.com

[c]School of Chemical and Biological Engineering, Changsha University of Science & Technology, Changsha, Hunan 410076, P. R. China.

Notes

Electronic Supplementary Information (ESI) available: ^{1}H NMR spectrum of **1** in DMSO-d_6. FT-IR spectra of **1**, **2** and **2-non**. Thermogravimetric curve of **2**. The fluoresence spectra of **2-non** interacting with (A) α-CD (B) β-CD and then with DNA (left inset, dotted lines). The fluoresence spectra of **1** interacting with (A) α-CD (B) β-CD and then with DNA (left inset, dotted lines). *See DOI: 10.1039/b000000x/*

References

1 K. Zhu, X. Y. Hu, Q. Y. Ge, Q. J. Sun, *Anal. Chim. Acta.*, 2014, **812**, 199.
2 S. Ghosh, K. B. Ucer, Jr. R. D'Agostino, K. Grant, J. Sirintrapun, M. J. Thomas, R. Hantgan, M. Bharadwaj, W. H. Gmeiner, *Nanomed.-Nanotechnol.*, 2014, **10**, 451.
3 B. Jin, H. M. Lee, Y. A. Lee, J. H. Ko, C. Kim, S. K. Kim, *J. Am. Chem. Soc.*, 2005, **127**, 2417.
4 R. J. Fiel, *J. Biomol. Struct. Dyn.*, 1989, **6**, 1259.
5 M. A. Bork, C. G. Gianopoulos, H. Y. Zhang, P. E. Fanwick, J. H. Choi, D. R. McMillin, *Biochemistry*, 2014, **53**, 714.
6 J. Manono, P. A. Marzilli, L. G. Marzilli, *Inorg. Chem.*, 2009, **48**, 5636.
7 G. P. Liu, Y. M. Wu, Y. L. Yuan, Y. Q. Chai, S. Q. Wei, D. J. Zhang, *RSC Adv.*, 2014, **4**, 52117.
8 Y. F. Li, C. R. Geyer, D. Sen, *Biochemistry*, 1996, **35**, 6911.
9 R. C. Haushalter, R. W. Rudolph, *J. Am. Chem. Soc.*, 1978, **100**, 4628.
10 J. Winkelman, *Cancer Res.*, 1962, **22**, 589.
11 F. Niedercorn, *New J. Chem.*, 1988, **12**, 897.
12 R. Lauceri, R. Purrello, S. J. Shetty, M. Gracüa, H. Vicente, *J. Am. Chem. Soc.*, 2001, **123**, 5835.
13 A. D'Urso, A. Mammana, M. Balaz, A. E. Holmes, N. Berova, R. Lauceri, R. Purrello, *J. Am. Chem. Soc.*, 2009, **131**, 2046.
14 J. K. Choi, A. D'Urso, M. Balaz, *J. Inorg. Biochem.*, 2013, **127**, 1.
15 M. Zheng, A. Jagota, M. S. Strano, A. P. Santos, P. Barone, S. G. Chou, B. A. Diner, M. S. Dresselhaus, R. S. McLean, G. B. Onoa, G. G. Samsonidze, E. D. Semke, M. Usrey, D. J. Walls, *Science*, 2003, **302**, 1545.
16 H. B. Zhao, H. K. Wang, H. Chang, S. J. Qiu, B. Y. Deng, J. X. Liao, *Chin. J. Chem.*, 2011, **29**, 1901.
17 H. Zhang, H. B. Zhao, X. J. Lu, W. L. Wang, H. Chang, Y. F. Wang, *Acta. Chim. Sinica*, 2011, **69**, 316.
18 D. Baskaran, J. W. Mays, X. P. Zhang, M. S. Bratcher, *J. Am. Chem. Soc.*, 2005, **127**, 6916.
19 Y. Wang, A. H. Zhou, *J. Photochem. Photobio. A: Chem.*, 2007, **190**, 121.
20 W. L. Wang, H. B. Zhao, J. H. Ning, Y. Hu, X. J. Lu, *J. Anal. Sci*., 2011, **27**, 183-1 86.
21 Y. Hu, H. B. Zhao, J. H. Ning, M. X. Ning, Y. J. Xu, S. J. Qiu, J. X. Liao, *Huaxue Xuebao*, 2008, **66**, 2391.
22 S. Li, W. G. Purdy, *Chem. Rev.*, 1992, **92**, 1457.
23 R. H. Yang, K. A. Li, K. M. Wang, N. Li, F. Zhao, F. Liu, *Anal. Chem*., 2003, **75**, 612.
24 D. Pantarotto, R. Singh, D. McCarthy, M. Erhardt, J. P. Briand, M. Prato, K. Kostarelos, A. Bianco, *Angew. Chem.*, 2004, **116**, 5354.
25 J. Carlstedt, D. Lundberg, R. S. Dias, B. Lindman, *Langmuir*, 2012, **28**, 7976.
26 W. J. Kruper, T. A. Chamberlin, M. Kochanny, *J. Org. Chem.*, 1989, **54**, 2753.
27 D. M. Guldi, G. M. A. Rahman, N. Jux, N. Tagmatarchis, M. Prato, *Angew. Chem. Int. Ed.*, 2004, **43**, 5526.
28 G. C. Catena, F. V. Bright, *Anal. Chem.*, 1989, **61**, 905.
29 X. M. Wang, D. L. Xu, *Iran J. Chem. Chem. Eng.*, 2013, **32**, 41.
30 R. F. Pasternack, C. Bustamante, P. J. Collings, A. Giannetto, E. J. Gibbs, *J. Am. Chem. Soc.*, 1993, **115**, 5393.
31 R. F. Pasternack, P. J. Collings, *Science*, 1995, **269**, 935.

Table of Contents

Novel supramolecular assemblies of repulsive DNA-anionic porphyrin complexes based on covalently modified multi-walled carbon nanotubes and cyclodextrins

Jingheng Ning, Yufang Wang, Qi Wu, Xuefeng Zhang, Xianfu Lin* and Hongbin Zhao

The strategy for constructing novel DNA-anionic porphyrin supramolecular assemblies by the "fixation" of CNTs and the "inclusion" of CDs was reported.